Density measurement of shock compressed foam using two-dimensional x-ray radiography

Sebastien Le Pape,[1] Andrew Macphee,[1] Daniel Hey,[1] Pravesh Patel,[1] Andrew Mackinnon,[1] Mike Key,[1] John Pasley,[2] Mingsheng Wei,[2] Sophia Chen,[2] Tammy Ma,[2] Farhat Beg,[2] N. Alexander,[3] Rich Stephens,[3] Dustin Offerman,[4] A. Link,[4] Lynn Van-Woerkom,[4] and R. Freeman[4]

[1]*Lawrence Livermore National Laboratory, 700 East Avenue, Livermore, California 94550, USA*
[2]*University of California San Diego, La Jolla, California 92093-0417, USA*
[3]*General Atomics, California 92121-1122, USA*
[4]*Ohio State University, Columbus, Ohio 43210, USA*

(Received 18 April 2008; accepted 25 August 2008; published online 10 October 2008)

We have used spherically bent quartz crystal to image a laser-generated shock in a foam medium. The foam targets had a density of 0.16 g/cm^3 and thickness of 150 μm, an aluminum/copper pusher drove the shock. The experiment was performed at the Titan facility at Lawrence Livermore National Laboratory using a 2 ns, 250 J laser pulse to compress the foam target, and a short pulse (10 ps, 350 J) to generate a bright Ti $K\alpha$ x-ray source at 4.5 keV to radiograph the shocked target. The crystal used gives a high resolution ($\sim$20 μm) monochromatic image of the shock compressed foam. © *2008 American Institute of Physics.* [DOI: 10.1063/1.2982237]

Foams have found a large number of applications especially in inertial confinement fusion (ICF) and astrophysics. In laboratory astrophysics experiments foams allow the study of supercritical radiative shocks due to the large heating of the foam induced by compression and to the long mean free path of radiation in the low-density material.[1,2] In indirect drive ICF, foams have been suggested as an alternative to the use of gas-filled holhraums to prevent the hydrodynamic expansion of the wall material.[3] Due to such large interest, there is a need for a precise characterization of foam materials under the action of intense laser light generating pressures in the megabar range and, in particular, there is a need to obtain equation-of-state (EOS) data for foams along the Hugoniot, i.e., under the action of an intense shock.

In the past few years several works have demonstrated the validity of shock wave experiment as a tool for EOS studies. This approach requires that two parameters, usually the shock and fluid velocity, are measured to infer the thermodynamics properties of the material. Only a few experiments have been carried out to study foam EOS and opacities.[4,5] The impedance mismatch technique has been used in foam EOS experiments. In this technique, the determination of only the velocity of the shock leads to a large error in the determination of the density as a consequence of error amplification through the Rankine–Hugoniot equations. The Rankine–Hugoniot equations are composed of three equations with five unknown parameters. These relations give the error resulting in the determination of the density

$$\Delta\rho = \rho_0 \left[\frac{u\Delta D + D\Delta u}{(D-u)^2} \right],$$

with U and D being the fluid and shock velocity measured.

This error is greatly larger to the error given by a direct measurement of the density using x-ray radiography. X-ray radiography is one of the main techniques used for imaging various stages of hydrodynamics. Until recently, hydrodynamic experiments utilized x-ray backlighters[6,7] based on thermal emission from laser-generated plasmas. Some recent experiments have used $K\alpha$ radiation from the interaction of a short pulse with matter.[8] In these experiments, the emitted light is polychromatic which makes the analysis more difficult to perform. In this paper, we present two-dimensional (2D) x-ray monochromatic images of shocked foam obtained with a high temporal resolution.

The interaction of an ultrahigh-intensity laser ($>10^{17}$ W/cm^2) produces $K\alpha$ fluorescence x rays from the interaction between hot electrons and cold atoms. This technique provides a better temporal resolution ($<$10 ps) and readily achieves the brightness required for high definition radiography.[9,10] The short duration of the $K\alpha$ x-ray source reduces the blurring due to the shock velocity to a value well below the spatial resolution of the imaging, for example, a typical shock of velocity 20 km/s travels only 0.2 μm in 10 ps while the spatial resolution of the imaging optic is 24 μm.

The experiment was performed on the Titan facility at the Lawrence Livermore National Laboratory.[11] The experimental setup is presented in Fig. 1. The short pulse beam, 270 J in 10 ps at 1.053 μm, is focused by a $f/3$ off-axis parabola on a titanium foil to generate an extended source of $K\alpha$ photons. The titanium foil is placed at an out-of-focus plane to produce a focal spot of 700×210 μm^2 full width at maximum with an average intensity of 1.6×10^{16} W/cm^2. This source foil was located 2 mm from the target and irradiated on its opposite side to the target. The long pulse target is composed of an ablator pusher comprised of 21 μm Al/4.2 μm Cu. The shock then propagates in a 150 μm layer of 0.16 g/cm^3 carbonized resorcinol formaldehyde (CRF) foam 3.9 μm. Au is glued to the back of the foam layer for a relativistic electron transport experiment, which is not discussed here. The long pulse used to generate the shock had a 2 ns square temporal profile and is able to deliver 250 J at 0.53 μm, the second harmonic wavelength.

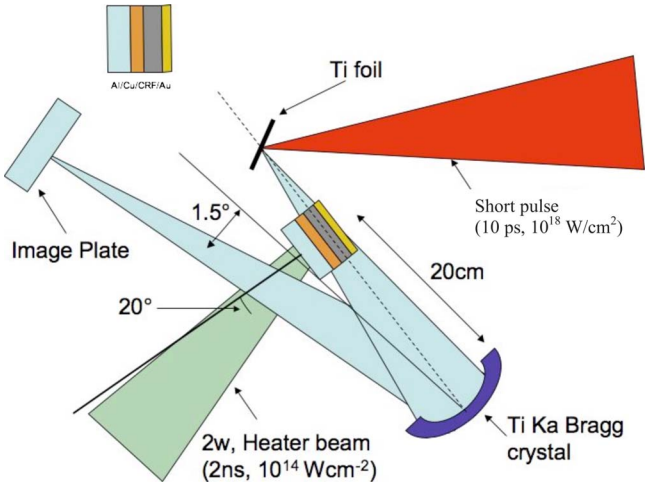

FIG. 1. (Color online) Schematic of the experimental arrangement.

The timing between the short and the long pulse that drives the shock has a 150 ps jitter.

A phase zone plate (PZP) is used to generate a flat focal spot of 200 μm diameter; the resulting intensity of the target is $\sim 10^{14}$ W/cm^2. A 1.6 cm aperture SiO_2 2023 quartz crystal bent to a radius of 38 cm and operating at 1° off normal incidence imaged a plane centered in the shocked target.[12] It produces an 11× magnified image onto an image plate (Fuji BAS-MS2025) via a 500 μm beryllium filter placed in front of the image plate. The resolution was tested using a 300 lpi (lines per inch) mesh placed at the position of the long pulse target; the resolution achieved is 24 μm.

Figure 2 shows a backlit image of an unshocked target. The pusher made of aluminum and copper is opaque to the 4.5 keV x rays. Similarly, gold at the back surface target is opaque to 4.5 keV photons. The transmission of the cold foam is measured from the lineout in Fig. 2(b). The target width of 600 μm and the CRF foam density of 0.16 g/cm^3 gives an opacity of 31 cm/g. The theoretical opacity given by the center for x-ray optics (CXRO) (Ref. 13) is

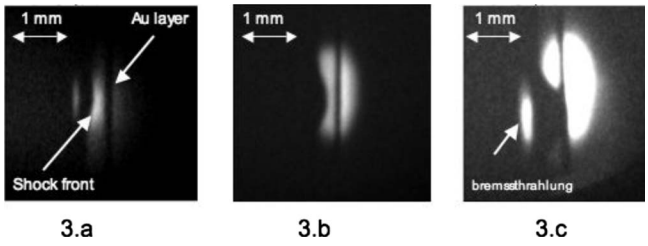

FIG. 3. Images of the shock at different time delays, the laser comes from the left. (a) 2.7 ns, (b) 4.2 ns, and (c) 6.2 ns. The spot of the left part of the image is due to the bremsstrahlung caused by the interaction of the long pulse laser with the pusher.

33 cm^2/g cm^3; it agrees within 10% with the experimental value. The small difference is presumably due to the presence of an oxide layer on the side of the target that modifies the transmission of the foam.

The shock propagation in the foam was imaged at 2.7, 4.2, and 6.2 ns delay. Figure 3 shows the shock at these times. The pusher propagating in the foam is clearly visible since it is opaque to 4.5 keV x rays. At 6.2 ns, the shock has reached the gold layer at the back of the target. The backlighter intensity profile is fitted using a hypergaussian. The absorption of x ray in matter is given by the Beer–Lambert law, $I=I_o*\exp(-\mu\rho z)$, where μ is the opacity, z is the path length, and ρ is the density. The cold value of the opacity is used in calculations since the temperature in the shock is below 30 eV, which does not change significantly the value of the opacity.

The use of PZP phase plate creates a symmetrical focal spot for the shock driver that allows the use of the Abel inversion technique. A three-point Abel deconvolution technique algorithm is used.[14] The Abel inversion technique being sensitive to the noise, the data have to be fit by a polynomial function. Figure 4 shows the resulting Abel inverted density profile at 4.2 ns. Various profiles have been taken at different positions in the shock front given the density profile in the whole shock front. The density profile is peaked at the

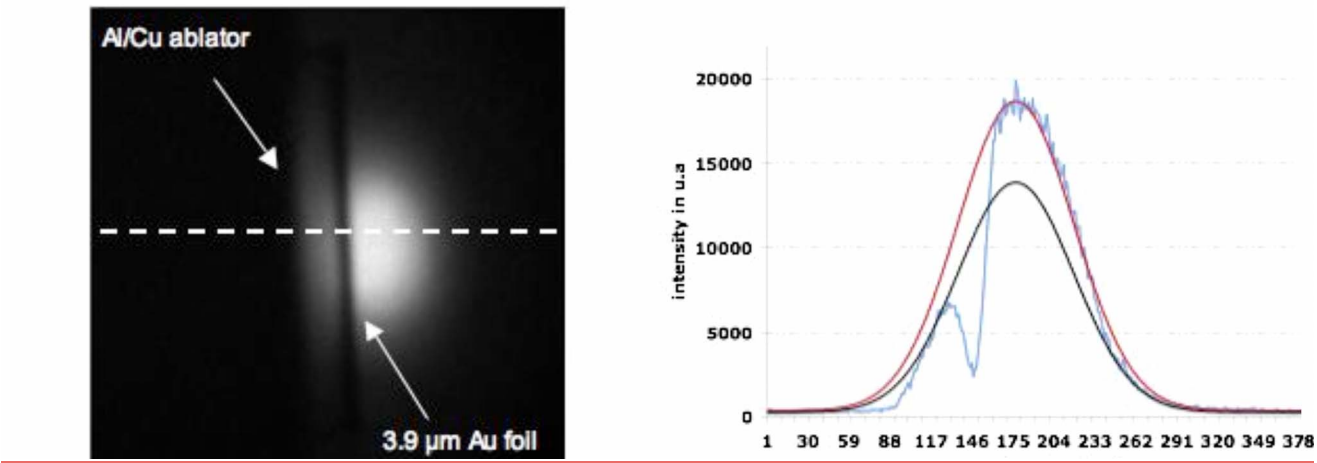

FIG. 2. (Color online) Radiography of the unshocked target. The left part of the line-out (indicated by the horizontal line through the image) is attenuated part on the signal due to the cold foam; the right part on the line-out is the nonattenuated part on the signal. The signal is fitted using a hyper-Gaussian either attenuated or not.

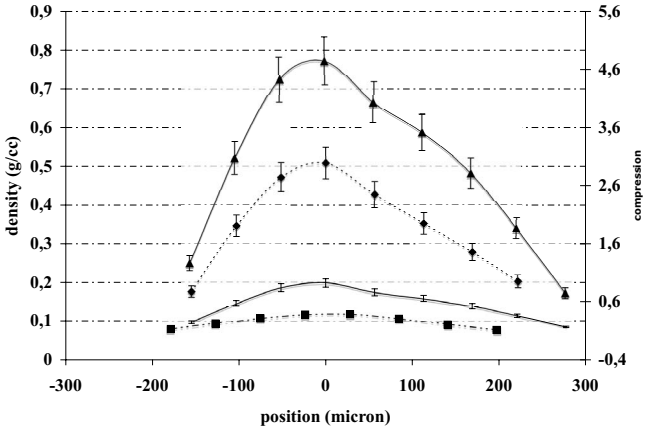

FIG. 4. Density and compression profiles along the shock front. 10 μm from the pusher (black diamond), 20 μm (dashed curve black circle), 30 μm (black curve), and 40 μm (black curve black square) from the pusher. The compression is calculated black diamond curve.

shock front and rapidly decreases when going toward the symmetry axis. This decrease is due to the spatial profile of the long pulse focal spot. The maximum of the density is 0.92 ± 0.12 g/cm^3, which corresponds to a compression of 5.6 ± 0.78. This value of the peak density does not reflect the value of the density in the shock front but the result of the convolution of the density profile with the resolution of the crystal imager (24 μm).

We have modeled our experiment using a 2D radiation-hydrodynamics code h2d.[15] In simulations, we used the laser parameters of 250 J in 2 ns in a 200 μm focal spot. The code correctly models the position of the pulse at different time delays; at 4.2 ns the shock front has traveled 100 μm in the foam on the image. This leads to a mean velocity of the shock in the foam of 24 km/s. The simulation gives a pusher position of 130 μm at 4.2 ns, which is in good agreement with the experimental data.

In conclusion we used a crystal at 4.5 keV imager to imager the propagation of a aluminum/copper pusher in a foam medium. Images have been made at different times of the pusher propagation in the foam. Its position as a function of time is in good agreement with 2D radiation-hydrodynamics simulations. This technique provides high quality data about the propagation of a laser-generated shock in a foam medium. It will give us crucial data in the very challenging study of EOS of foam medium.

This work was performed under the auspices of the U.S. Department of Energy under Contract Nos. DE-FC02-04ER54789 (Fusion Science Center), DE-FG02-05ER54834, and W-7405-Eng-48. The work and vital assistance of the technical, scientific, and administrative staff connected with the Jupiter Laser Facility at LLNL are gratefully acknowledged. Useful discussions regarding these experiments with S. C. Wilks of LLNL are also kindly acknowledged. This experiment was performed as part of LLNL's Institute of Laser Science and Applications-University Program.

[1] Y. B. Zeldovich and Y. P. Raizer, *Physics of Shock Waves and High Temperature Hydrodynamic Phenomena* (Academic, New York, 1967).
[2] B. Remington, J. Kane, R. P. Drake, S. G. Glendinning, K. Estabrook, R. London, J. Castor, R. J. Wallace, D. Arnett, E. Liang, R. McCray, A. Rubenchik, an dB. Fryxell, Phys. Plasmas **4**, 1994 (1997); R. P. Drake, S. G. Glendinning, K. Estabrook, B. A. Remington, R. McCray, R. J. Wallace, L. J. Suter, T. B. Smith, J. J. Carroll, III, R. A. London, and E. Liang Phys. Rev. Lett. **81**, 2068 (1998); J. Massen, G. D. Tsakiris, K. Eidmann, I. B. Földes, Th. Löwer, R. Sigel, S. Witkowski, H. Nishimura, T. Endo, H. Shiraga, M. Takagi, Y. Kato, S. Nakai, Phys. Rev. E **50**, 5130 (1994).
[3] M. Desselberger, M. W. Jones, J. Edwards, M. Dunne, and O. Willi, Phys. Rev. Lett. **74**, 2961 (1995); R. G. Watt, D. C. Wilson, R. E. Chrien, R. V. Hollis, P. L. Gobby, R. J. Mason, R. A. Kopp, R. A. Lerche, D. H. Kalantar, B. MacGowan, M. B. Nelson, T. Phillips, P. W. Mckenty, and O. Willi, Phys. Plasmas **4**, 1379 (1997).
[4] A. Benuzzi-Mounaix, M. Koenig, A. Ravasio, T. Vinci, N. Ozaki, M. Rabec le Gloahec, B. Loupias, G. Huser, E. Henry, S. Bouquet, C. Michaut, D. Hicks, A. MacKinnon, P. Patel, H. S. Park, S. LePape, T. Boehly, M. Borghesi, C. Cecchetti, M. Notley, R. Clark, S. Bandyopadhyay, S. Atzeni, A. Schiavi, Y. Aglitskiy, A. Faenov, T. Pikuz, D. Batani, R. Dezulian, and K. Tanaka, Plasma Phys. Controlled Fusion **48**, B347 (2006).
[5] F. Philippe, B. Canaud, X. Fortin, F. Garaude, and H. Jourdren, Laser Part. Beams **22**, 171 (2004).
[6] D. Hoarty, O. Willi, L. Barringer, C. Vickers, R. Watt, and W. Nazarov, Phys. Plasmas **6**, 2117 (1999); R. P. Drake, S. G. Glendinning, K. Estabrook, B. A. Remington, R. McCray, R. J. Wallace, L. J. Suter, T. B. Smith, J. J. Carroll III, R. A. London, and E. Liang, Phys. Rev. Lett. **81**, 2068 (1998).
[7] A. Benuzzi-Mounaix, B. Loupias, M. Koenig, T. Vinci, M. Rabec, L. Gloahec, A. Ravasio, N. Ozaki, Y. Aglitskiy, A. Faenov, and T. Pikuz, Plasma Phys. Controlled Fusion **48**, B347 (2006).
[8] A. Ravasio, Proceedings of the Workshop on Warm Dense Matter, Porquerolles, France, June 2007 (unpublished).
[9] H.-S. Park, N. Izumi, M. H. Key, J. A. Koch, O. L. Landen, P. K. Patel, T. W. Phillips, and B. B. Zhang, Rev. Sci. Instrum. **75**, 4048 (2004).
[10] J. A. King, K. Akli, B. Zhang, R. R. Freeman, M. H. Key, C. D. Chen, S. P. Hatchett, J. A. Koch, A. J. MacKinnon, P. K. Patel, R. Snavely, R. P. J. Town, M. Borghesi, L. Romagnani, M. Zepf, T. Cowan, H. Habara, R. Kodama, Y. Toyama, S. Karsch, K. Lancaster, C. Murphy, P. Norreys, R. Stephens, and C. Stoeckl, Appl. Phys. Lett. **86**, 191501 (2005).
[11] G. Rennie, "Titan leads the way in laser-matter science," National Technical Information Service Document (2007).
[12] J. A. Koch, Y. Aglitskiy, C. Brown, T. Cowan, R. Freeman, S. Hatchett, G. Holland, M. Key, A. MacKinnon, J. Seely, R. Snavely, and R. Stephens, Rev. Sci. Instrum. **74**, 2130 (2003).
[13] CXRO, http://henke.lbl.gov/optical_constants/filter2.html.
[14] C. J. Dasch, Appl. Opt., **31**, 1146 (1992).
[15] h2d is a commercial product of Cascade Applied Sciences incorporated, 6325 Trevarton Drive, Longmont, CO 80503.